

Axisymmetric numerical modeling of a unit cell in geosynthetic-reinforced, column-supported embankments

M. Smith¹ and G. Filz²

¹Research and Consulting Engineer, Swedish Geotechnical Institute, SE-581 93 Linköping, Sweden, Telephone: +46 13 20 18 22, Telefax: +46 13 20 19 14, E-mail: miriam.smith@swedgeo.se

²Professor, Department of Civil and Environmental Engineering, Virginia Tech, Blacksburg, VA 24061, USA, Telephone: +540 231 7151, Telefax: +540 231 7532, E-mail: filz@vt.edu

Received 15 May 2006, revised 27 September 2006, accepted 27 September 2006

ABSTRACT: Rational design of geosynthetic-reinforced, column-supported embankments requires realistic estimates of the portion of the embankment load that acts vertically downward on the geosynthetic in the area underlain by the foundation soil located between columns. This vertical load can then be used to calculate the strain and tension that develops in the plane of the geosynthetic reinforcement. Several simplified methods are available for calculating the vertical load acting on the geosynthetic, but these methods produce dramatically different results, and there is not agreement regarding which method produces the best estimates. Axisymmetric numerical modeling provides an alternative approach for determining the vertical stresses that develop in the embankment and act on the geosynthetic reinforcement. In this research, axisymmetric numerical modeling is verified against: (1) instrumentation data from a full-scale column-supported test embankment, albeit without geosynthetic reinforcement, at the I-95/Route 1 Interchange project in Virginia, USA; (2) an analytic solution for a disk of membrane material that is pinned at its outer edge and subject to a vertical stress; (3) instrumentation data from a pilot-scale test of a geosynthetic-reinforced, column-supported embankment conducted at the University of Kassel in Germany; and (4) three-dimensional numerical analyses. The results demonstrate that drained axisymmetric numerical analyses using a mesh of linear elastic zones to represent the geosynthetic reinforcement produce results in good agreement with instrumentation data, the analytic solution, and three-dimensional analyses.

KEYWORDS: Geosynthetics, Numerical modeling, Column-supported embankment, Axisymmetric, Field test, Scaled laboratory test, FLAC, FLAC3D, SAGE

REFERENCE: Smith, M. & Filz, G. (2007). Axisymmetric numerical modeling of a unit cell in geosynthetic-reinforced, column-supported embankments. *Geosynthetics International*, **14**, No. 1, 13–22

1. INTRODUCTION

Columnar support can be used to reduce settlement and improve the stability of embankments placed on soft ground. The columns can be driven piles, deep-mixing-method columns, or other types of column. Layers of geosynthetic reinforcement are often used in the bottom of the embankment to help transfer the embankment load to the columns. An important part of the design process for these systems is to estimate the portion of the embankment load that is carried by the geosynthetic spanning between columns. Several different methods exist for calculating this load (e.g. BS 8006 1995; Russell and Pierpoint 1997; Rogbeck *et al.* 1998; Russell *et al.* 2003; Collin 2004; Kempfert *et al.* 2004). These methods take into account such factors as the column or pile cap size,

column spacing, embankment height, embankment unit weight, and embankment friction angle, and they can produce loads that differ by an order of magnitude or more for typical examples (Russell and Pierpoint 1997; Kempton *et al.* 1998; Habib *et al.* 2002; Horgan and Sarsby 2002; Stewart and Filz 2005).

Because the existing methods produce such different results, it is important to gain an understanding of the load transfer mechanisms involved so that reliable estimates of the load on the geosynthetics can be used for design. Data from instrumented field cases and pilot-scale tests are helpful in this regard. Numerical analyses can also be used to calculate the loads on geosynthetic reinforcement. Verified numerical methods are particularly useful for performing parameter studies to determine the influences

that various components have on system response. However, geosynthetic-reinforced, column-supported embankments are complex three-dimensional systems, and three-dimensional numerical modeling requires substantial time to set up the problem and perform the calculations. In addition, modeling the out-of-plane behavior of geosynthetic reinforcement in three-dimensional models can be challenging. Russell and Pierpoint (1997) used a system of cable elements in FLAC3D (Fast Lagrangian Analysis of Continua in 3 Dimensions) (Itasca 2002a) to model a geogrid layer at the bottom of an embankment. Their model used displacement restraints to represent columns, and it did not include any foundation soil. Plaxis3D (Brinkgreve and Broere 2004) is not able to automatically capture the out-of-plane response of a geogrid because it does not provide for updating the mesh geometry, which is necessary to model the ‘trampoline’ effect of the geogrid.

If it can be verified that two-dimensional axisymmetric analyses are appropriate for modeling geosynthetic-reinforced, column-supported embankments, the benefits would include reduced time to set up numerical models and perform the calculations. This would permit investigation of a wide range of parameter values to determine the influence of the various system components on performance. The main objective of the current paper is to demonstrate that, for the purpose of determining average vertical stresses applied by an embankment to geosynthetic reinforcement, axisymmetric modeling is effective, and that the geosynthetic material can be represented by a grid of linear-elastic mesh zones.

It is important to distinguish between the vertical stresses acting down on the geosynthetic and the strains and tensions that develop in the plane of the geosynthetic. Although axisymmetric numerical analyses can produce good estimates of the average vertical stresses acting on the geosynthetic, either three-dimensional numerical analysis or a simplified mathematical model is necessary to calculate the strains and tensions that develop in orthotropic geosynthetic reinforcement.

The following sections describe the axisymmetric approximation of the full three-dimensional problem, axisymmetric modeling of a column-supported embankment without geosynthetic reinforcement, numerical modeling of an axisymmetric membrane, axisymmetric modeling of a pilot-scale column-supported embankment with geosynthetic reinforcement, and comparisons between axisymmetric and three-dimensional numerical modeling of an example column-supported embankment with geosynthetic reinforcement. The final section presents a summary and conclusions regarding the suitability of axisymmetric modeling for geosynthetic-reinforced, column-supported embankments.

2. AXISYMMETRIC APPROXIMATION OF THE THREE-DIMENSIONAL PROBLEM

Geosynthetic-reinforced, column-supported embankments are complex, three-dimensional systems that require three-dimensional modeling for complete representation. For the

interior portions of embankments, away from the influence of the embankment side slopes, much work has been based on the ‘unit cell’ concept (BS 8006 1995; Russell and Pierpoint 1997; Kempton *et al.* 1998; Han and Gabr 2002). Figure 1 shows a unit cell in plan and elevation views, together with the minimum representative region necessary for three-dimensional analyses. The minimum representative region is bounded by three vertical planes of symmetry, for which there are no horizontal displacements in directions perpendicular to the symmetry planes and no shear stresses on the symmetry planes. Thus the appro-

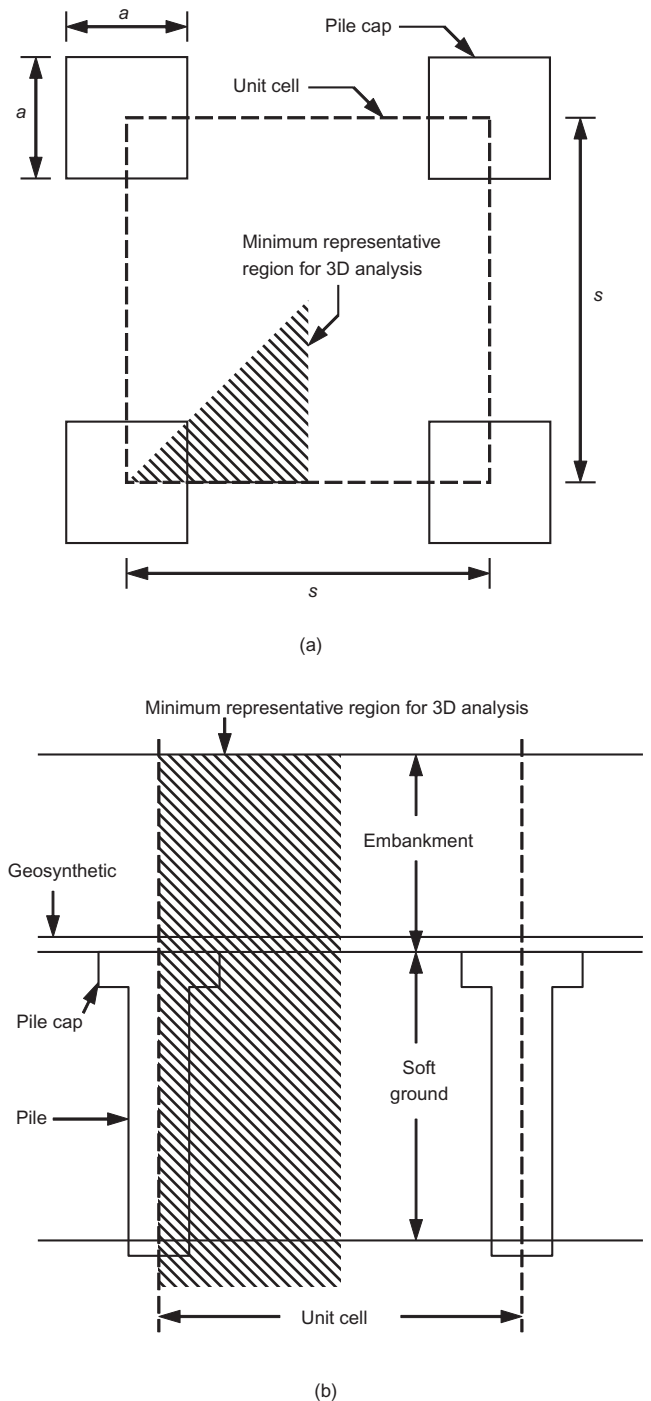


Figure 1. Unit cell in a column-supported embankment: (a) plan; (b) elevation

priate boundary conditions on these planes are rollers that permit in-plane movement but no out-of-plane movement.

An axisymmetric approximation of the minimum representative region for three-dimensional analyses is shown in Figure 2. The axisymmetric dimensions are selected to produce exactly the same area for the pile cap and the soil, so that the resulting area replacement ratio is also the same. The boundary conditions for the axisymmetric approximation are just like those for the three-dimensional representation, with rollers automatically in effect on the two radial planes and rollers imposed on the outer arc. A pie-shaped section of an axisymmetric model is shown in Figure 2 to facilitate comparison with the three-dimensional representation, but only axial and radial deflections are calculated in the two-dimensional axisymmetric analyses because the circumferential deflections are all zero.

Figure 2 also shows a comparison between the minimum three-dimensional representation and the axisymmetric representation of the unit cell. For systems without geosynthetics, or with isotropic geosynthetics, the only differences between the two representations are in the shape of the pile/soil contact and the shape of the boundary farthest from the center of the pile. Considering

the similarity of the axisymmetric and three-dimensional representations, it is difficult to imagine that there would be much difference between the calculated values of average vertical stress applied to the geosynthetic reinforcement in the area underlain by soft ground using these two different representations of the unit cell.

Figures 1 and 2 show square pile caps. Embankments can also be supported on round columns, such as those produced by the deep mixing method. If round columns are used, differences between the three-dimensional and axisymmetric representations of the unit cell are even smaller than if square piles or pile caps are used.

As shown in the following sections, axisymmetric analyses produce realistic values of the vertical stress developing in the embankment and acting on geosynthetic reinforcement in the portion of the unit cell underlain by the foundation soil between columns. However, axisymmetric modeling cannot fully represent orthotropic geosynthetic reinforcement or the stress concentration expected in the geosynthetic at the corner of a square pile cap. To fully represent these conditions, three-dimensional numerical modeling is necessary. One alternative to performing three-dimensional numerical analyses is to

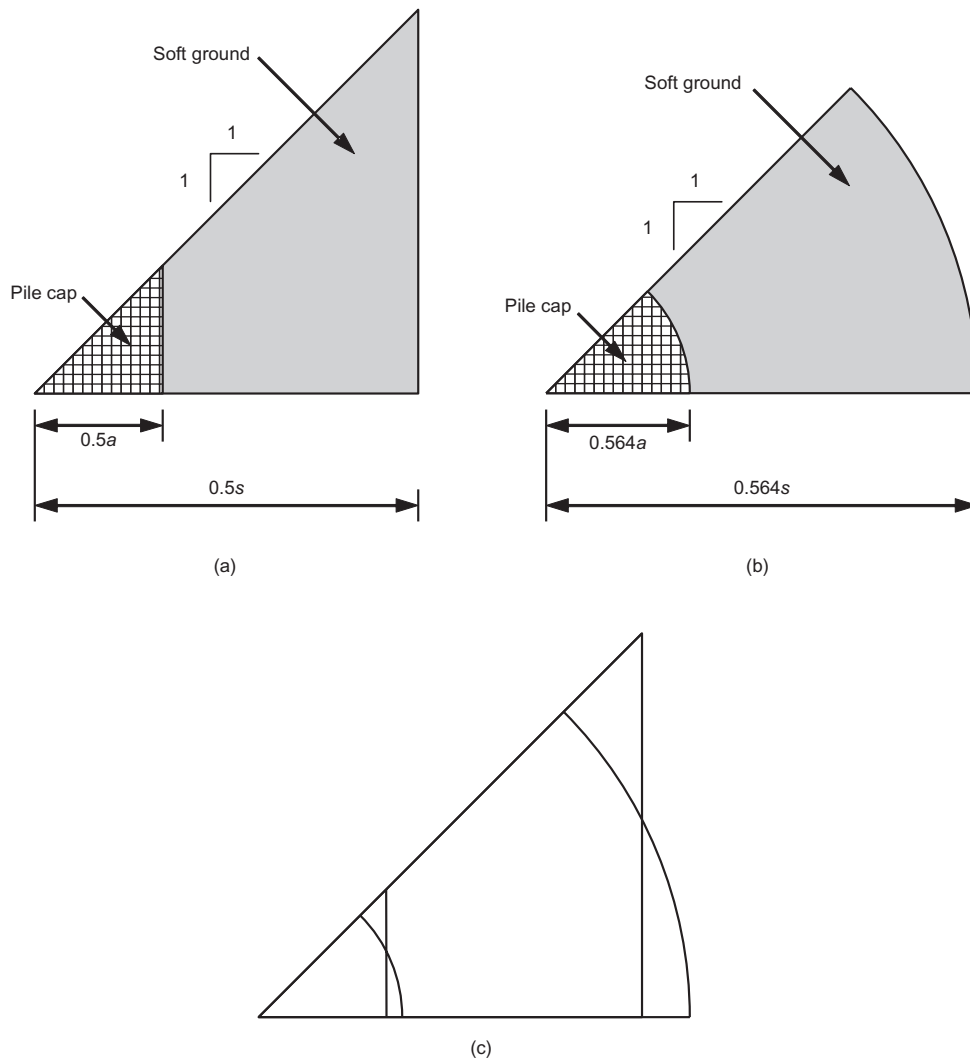


Figure 2. Comparison of representative three-dimensional and axisymmetric regions: (a) representative region for 3D analysis; (b) representative region for axisymmetric analysis; (c) comparison of representative regions

first determine the vertical stress acting on the geosynthetic reinforcement using axisymmetric numerical analyses and then apply an approach based on BS 8006 (1995) to calculate the strain and tension in the geosynthetic reinforcement.

In the BS 8006 method for calculating the strain and tension in the geosynthetic reinforcement, the load acting on the shaded area in Figure 3 is assumed to be carried by the portion of the geosynthetic reinforcement that spans directly between columns. This portion of the geosynthetic reinforcement is assumed to deform as a parabola. The strain in the geosynthetic reinforcement, ϵ_g , can be obtained by solving the following cubic equation:

$$96\epsilon_g^3 - 6K_g^2\epsilon_g - K_g^2 = 0 \tag{1}$$

where $K_g = p_{net}A_s/(J_g a)$, p_{net} is the average net vertical stress acting on the geosynthetic in the area not underlain by columns or pile caps, $A_s = s^2 - a^2$ is the portion of a unit cell not underlain by columns or pile caps, s is the center-to-center spacing of the columns or pile caps, a is the pile cap width, J_g is the geosynthetic stiffness = $E_g t$, E_g is the geosynthetic modulus, and t is the geosynthetic thickness. If round columns or pile caps with diameter d_c are used, then the value of a is set equal to $0.886d_c$ when evaluating K_g .

The tension in the geosynthetic reinforcement, T_g , is obtained by multiplying the strain, ϵ_g , by the stiffness, J_g .

3. AXISYMMETRIC MODELING OF A COLUMN-SUPPORTED EMBANKMENT WITHOUT GEOSYNTHETIC REINFORCEMENT

Verification analyses were performed to gain an understanding of the appropriate numerical modeling procedures and required mesh refinement for axisymmetric analyses of column-supported embankments (Stewart *et al.* 2004; Stewart and Filz 2005; Filz and Smith 2006). The results of the verification analyses were compared with measurements from an instrumented test embankment supported on deep-mixed soil-cement columns installed by the dry method at the interchange of US I-95 and Virginia State Route 1 in Alexandria, Virginia. The soil-cement columns are 810 mm in diameter and about 11 m long, extending through about 9.5 m of soft organic clay; they were installed in a triangular pattern on 1.83 m and 3.05 m center-to-center spacings, corresponding to

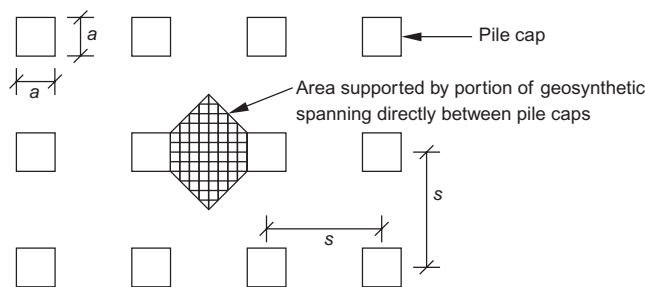


Figure 3. Area supported by geosynthetic spanning directly between columns

area replacement ratios of 17.9% and 6.4%, respectively, in two different areas beneath the 5.5 m high test embankment. Additional detailed descriptions of the site subsurface conditions, column construction methods, and embankment materials and geometry, as well as descriptions of the numerical analyses, can be found in Stewart *et al.* (2004) and Stewart and Filz (2005).

Two-dimensional, drained axisymmetric numerical analyses of the test embankment were performed using FLAC (Fast Lagrangian Analysis of Continua) (Itasca 2002b). The results of the two-dimensional model provided a good match to the pressure cell data, as shown in Figure 4. It can also be seen in Figure 4 that the stress concentration increases as the top of the column is approached from above.

In the drained numerical analyses, complete consolidation of the clay occurred as the embankment was placed in lifts. To investigate the impact that delayed consolidation would have on the calculated stress distribution in the embankment, water-soil coupled consolidation analyses of the I-95/Route 1 test embankment were also performed using the finite-element program SAGE (Static Analysis of Geotechnical Engineering Problems) (Bentler *et al.* 1999), which provides for efficient analysis of consolidation problems in two dimensions. First, an axisymmetric drained analysis was performed using SAGE, and the results are in excellent agreement with the FLAC analyses, as shown in Figure 4. Next, an axisymmetric consolidation analysis was performed using SAGE. Figure 5 shows that the results of the SAGE analyses after completion of consolidation are in very good agreement with the results of the SAGE drained analyses.

An interesting characteristic of the pressure cell readings at the I-95/Route 1 test embankment is that they responded almost immediately to fill placement, which occurred in about 10 days, and they did not change appreciably after that, even though the test embankment continued to settle for the approximately 13 months that the embankment was in place. This indicates that the local relative deformation pattern near the top of the columns was established very quickly, perhaps because of rapid consolidation of the soft soil near the top of the columns,

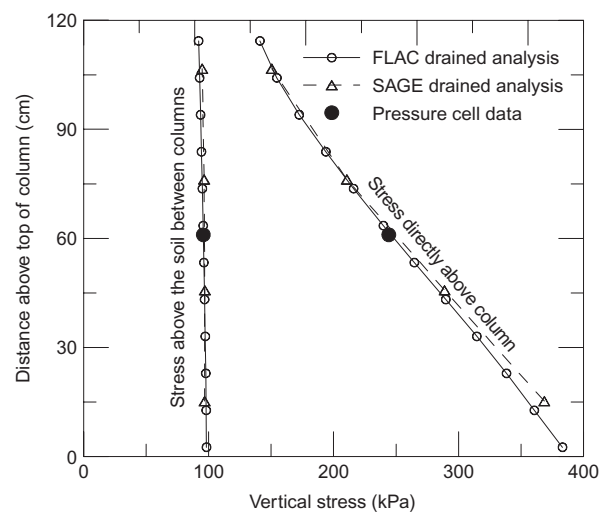


Figure 4. Comparison of axisymmetric numerical analyses with pressure cell data for the I-95/Route 1 test embankment

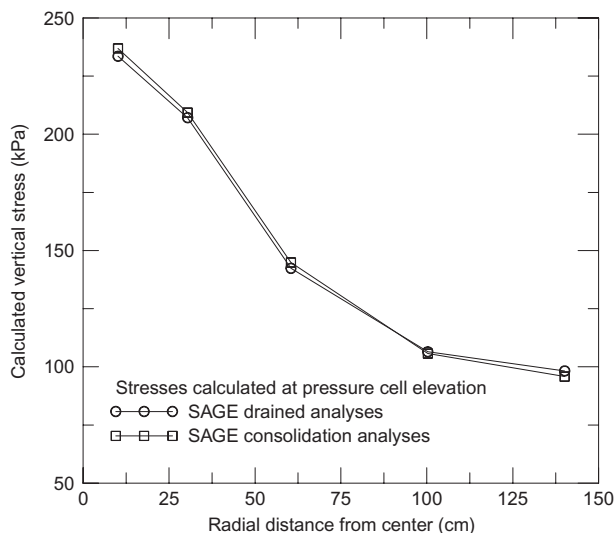


Figure 5. Comparison of axisymmetric SAGE drained and consolidation analyses

as would be expected near a drainage boundary. It appears in this case that ongoing consolidation of the soft soil at depth did not appreciably affect stress distribution at the level of the top of the columns.

The results of the FLAC and SAGE numerical analyses indicate that drained axisymmetric analyses provide good representation of stresses in embankments above soft ground that is reinforced with columns, at least for the conditions at the I-95/Route 1 interchange.

In addition to the axisymmetric analyses, three-dimensional drained analyses were performed using FLAC3D (Itasca 2002a). Two three-dimensional models were created based on: (1) the true three-dimensional geometry as illustrated in Figures 1 and 2a, except that the column tops are round; and (2) the three-dimensional 'axisymmetric' geometry as illustrated in Figure 2b. Results of the three-dimensional models produced good agreement with each other and with the axisymmetric FLAC analyses, as shown in Figure 6. These results show that not much is lost by

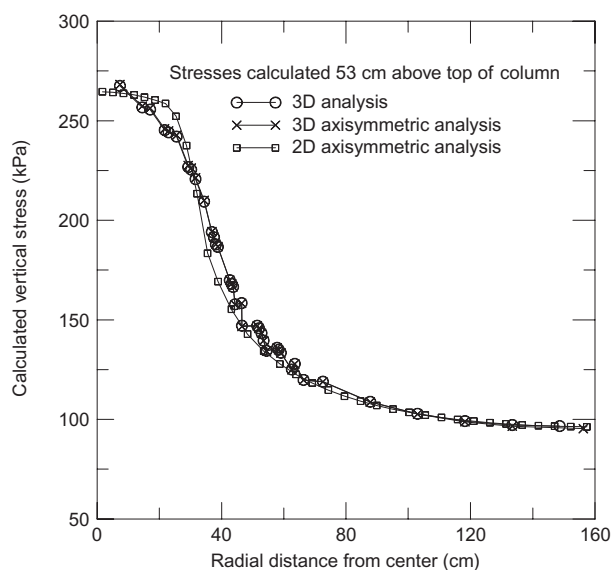


Figure 6. Comparison of two- and three-dimensional numerical analyses of the I-95/Route 1 test embankment

providing a curved boundary in the axisymmetric models, at least for column-supported embankments without geosynthetic reinforcement.

4. NUMERICAL MODELING OF AN AXISYMMETRIC MEMBRANE

The two-dimensional finite-difference computer program FLAC has several built-in structural elements. Beam elements are two-dimensional elements with three degrees of freedom at each end node, and they are used to represent a structural member in which bending resistance is important. Cable elements are one-dimensional axial elements that can support tension, but they cannot sustain a bending moment. In plane strain FLAC models, beam and cable elements may be used to model geosynthetic reinforcement; however, these structural elements cannot be used with axisymmetric models. Consequently, the suitability of a grid of linear elastic zones to represent geosynthetic reinforcement in a two-dimensional axisymmetric model was investigated by comparing the response of a grid of linear elastic zones to an analytic solution for a circular membrane subjected to a normal load. The outer diameter of the circular membrane is pinned, and the centerline edge of the mesh is allowed to deflect, as shown in Figure 7. The maximum deflection, w_{\max} , occurs at the centerline edge.

An analytical solution provided by Ugral (1999) was used to verify the results of the FLAC axisymmetric numerical analyses. For a pinned circular membrane with a Poisson's ratio of 0.3 subjected to a uniform vertical stress, Ugral (1999) presents the following solution:

$$w_{\max} = 0.704r \times \sqrt[3]{\frac{pr}{Et}} = 0.704a \times \sqrt[3]{\frac{pr}{J}} \quad (2)$$

where w_{\max} is the maximum deflection of the membrane that occurs at the center of the membrane, p is the applied uniform vertical load, r is the radius of the circular membrane, E is the membrane elastic modulus, t is the membrane thickness, and $J = Et$ is the stiffness of the membrane.

The grid of linear elastic material was divided into two layers, and it was subjected to uniform loads of 35, 105 and 140 kPa. Analyses were performed for three values of membrane radius: 30, 60 and 90 cm. The thickness of the membrane was set equal to 0.25 cm, and the elastic modulus was set equal to 584,000 kPa, which produces a value of J equal to 1460 kN/m. The results of the

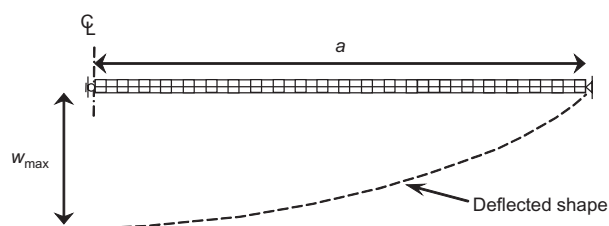


Figure 7. Schematic of axisymmetric numerical model of a disk of membrane material

axisymmetric FLAC verification study are summarized in Table 1 in terms of the normalized deflection, which is defined as the center deflection obtained from the FLAC analyses divided by w_{max} from Equation 2. The results in Table 1 show that the numerical calculations are within about 5% of the analytic solution in all cases. The degree of agreement improves as the normal pressure increases and the radius increases. It can also be seen that the results for mesh zone aspect ratios of 2:1 and 4:1 are about the same.

5. LABORATORY-SCALE MODEL TESTS

A very useful set of laboratory pilot-scale model tests were performed at the Institute of Geotechnics, University of Kassel, to evaluate the load transfer mechanisms of geosynthetic-reinforced, column-supported embankments. An abbreviated discussion of the model tests is provided in English by Kempfert *et al.* (2004), and a detailed description of the model tests is presented in the German dissertation by Zaeske (2001). The following sections describe the model configuration, the property values of the materials used in the model tests, and axisymmetric numerical analyses of the model tests.

5.1. Model test configuration

As described by Zaeske (2001) and Kempfert *et al.* (2004), a three-dimensional instrumented model was fabricated consisting of a group of four piles placed in a rectangular grid in a soft soil. The dimensions and configuration of the model are shown in Figure 8. The square piles had widths of 16 cm and center-to-center spacings of 50 cm, which correspond to an area replacement ratio of 10%. The thickness of the soft soil was 40 cm.

In separate experiments, sand was placed above the piles in two thicknesses: 35 cm and 70 cm. The sand thickness is represented by the variable H in Figure 8. One layer of geogrid was placed approximately 3 cm above the tops of the piles within the sand. For each thickness of sand, three static surcharge pressures were applied independently: 20, 54 and 104 kPa. In the model tests, the stress distribution resulting from static loading was meas-

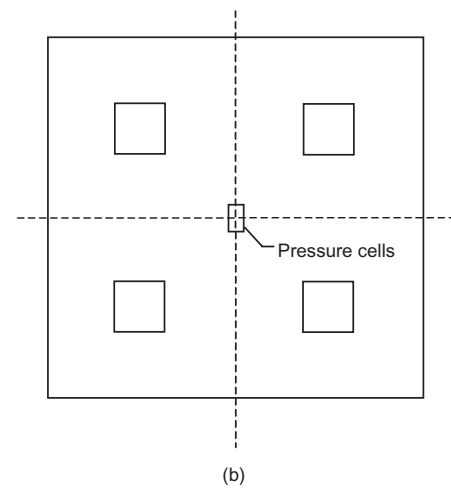
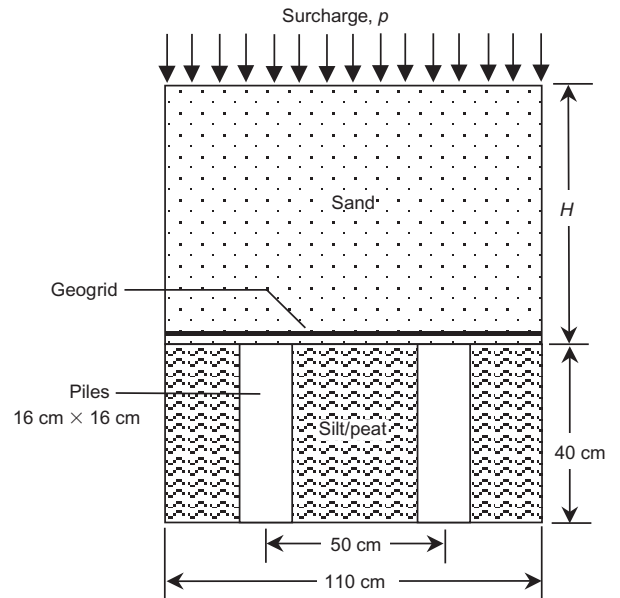


Figure 8. Model test dimensions and configuration: (a) section view; (b) plan view of piles

ured by pressure cells located at several elevations in the sand above the soft soil between columns.

5.2. Material property values

The Kempfert *et al.* (2004) reference does not include a discussion of the property values of the materials used in the model tests; however, a detailed description of the material property values is provided in the German dissertation by Zaeske (2001). Material property values were ascertained from the German text through the use of *Elsevier's Dictionary of Soil Mechanics in Four Languages*, and through personal conversations with Professor Rolf Katzenbach, of the Technische Universität Darmstadt, Frankfurt, Germany.

The soft soil has been referred to as both a silt (Zaeske 2001) and a peat (Kempfert *et al.* 2004). The soft soil between the piles was modeled using the Modified Cam Clay material model. The soft soil was assigned a buoyant unit weight of 8 kN/m³ and a saturated unit weight of 17.7 kN/m³. A specific gravity of 2.5 was assumed for the

Table 1. Normalized numerical calculation of the deflection of a disk of membrane material

p (kPa)	r (cm)	Mesh zone aspect ratio	
		2H:1V	4H:1V
35	30	0.945	0.951
105		0.958	0.961
140		0.963	0.966
35	60	0.949	0.951
105		0.972	0.972
140		0.981	0.982
35	90	0.954	0.953
105		0.982	0.985
140		0.994	0.998

soil, and, as a result, a void ratio of 0.85 was determined for the soft soil. Zaeske (2001) indicates that the compression and recompression indices of the soft soil are 2.48 and 0.5, respectively. These indices convert to values of the Cam Clay compressibility parameters λ and κ equal to 1.08 and 0.22, respectively. A Poisson's ratio of 0.38 was assumed for the soft soil.

A linear-elastic, perfectly plastic model with a Mohr–Coulomb failure criterion was used to model the sand. The sand has a moist unit weight of 17.6 kN/m³, a confined modulus of 28,000 kPa, an effective cohesion intercept of zero, and an effective friction angle of 38° (Zaeske 2001). A Poisson's ratio of 0.3 was assumed for the sand. Zaeske (2001) indicates that the sand also has a dilation angle of 11°; however, the best results were obtained in this study by assigning a dilation angle of zero to the sand.

The piles were modeled as a linear elastic material with an elastic modulus of 12.5×10^6 kPa and a Poisson's ratio value of 0.2.

The geogrid was modeled as a linear elastic material using two rows of mesh zones. The geogrid has a stiffness J of 1000 kN/m (Kempfert *et al.* 2004). The geogrid was assigned a thickness of 0.25 cm and a Poisson's ratio value of zero.

A summary of the property values used for the pile and soil materials in the numerical analyses is provided in Table 2.

5.3. Axisymmetric numerical analyses

Axisymmetric analyses of the pilot-scale tests were performed using FLAC. The square piles were converted to circular piles with equal areas, and the pile spacings were converted to circular areas while maintaining the same area replacement ratio, as illustrated in Figure 2. Accordingly, the 16 cm square pile was converted to a circular pile with a radius of 9.03 cm, and the total model radius was set equal to 28.22 cm.

Mesh refinement employed five zones across the radius

of the column, and nine zones across half the annulus of the soil between columns. Twenty layers of mesh zones were used in the vertical direction for the soft soil. The geogrid, which has an assigned thickness of 0.25 cm, was represented with two layers of mesh zones in the vertical direction. Sixteen layers of vertical mesh zones were used to represent the sand thickness of 35 cm, and 34 layers of vertical mesh zones were used to represent the sand thickness of 70 cm. For the full height of sand thickness of 70 cm, a total of 826 mesh zones were used.

Results from the FLAC analyses were compared with the results of the model tests, as published by Zaeske (2001) and Kempfert *et al.* (2004). Figures 9 and 10 show the stress distribution in the sand plotted against the distance above the top of the piles. It can be seen that the agreement between the measured and calculated values of vertical stress is good, especially for the lower surcharge pressures. It can also be seen that the values of vertical stress increase with elevation. This occurs because the pressure cells are located above the soft soil between columns, which compresses more than the stiff piles compress. This produces arching in the embankment fill, with reduced pressures above the soft soil and increased pressures above

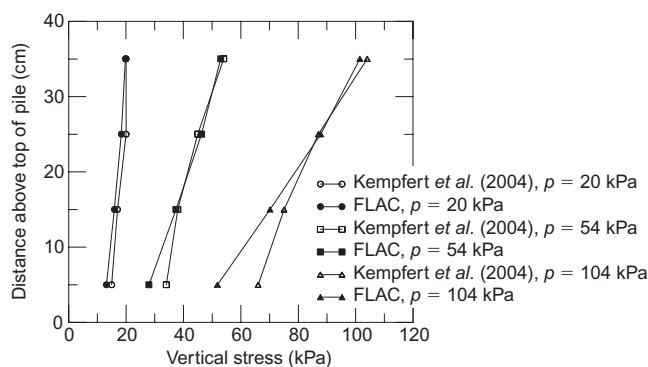


Figure 9. Stress distribution: axisymmetric FLAC analyses plotted against model tests ($H = 35$ cm)

Table 2. Summary of property values for the pile and soils used in verification study

Property	Pile	Silt/peat	Sand
	Model type		
	Linear elastic	Cam Clay	Linear-elastic, perfectly plastic, with Mohr–Coulomb failure criterion
Moist unit weight (kN/m ³)	23.5	–	17.6
Saturated unit weight (kN/m ³)	–	17.7	–
Young's modulus (kPa)	12.5×10^6	–	20,800
Poisson's ratio	0.2	0.38	0.3
Cohesion (kPa)	–	–	0
Friction angle (degrees)	–	–	38
Dilation angle (degrees)	–	–	0
Critical shear stress ratio, η_{crit}	–	1.1	–
λ	–	1.08	–
κ	–	0.22	–
Pressure at specific volume (kN/m ²)	–	16.5	–
Specific volume	–	1.85	–

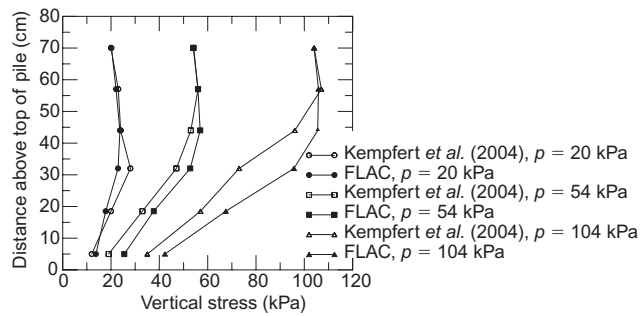


Figure 10. Stress distribution: axisymmetric FLAC analyses plotted against model tests ($H = 70$ cm)

the columns. The effect of stress concentrations decreases at greater elevations above the top of the pile caps.

6. COMPARISON BETWEEN AXISYMMETRIC AND THREE-DIMENSIONAL MODELING OF AN EXAMPLE GEOSYNTHETIC-REINFORCED, COLUMN-SUPPORTED EMBANKMENT

Two additional sets of analyses were performed to compare the results of axisymmetric analyses of unit cells in geosynthetic-reinforced, column-supported embankments with the results of corresponding three-dimensional analyses. In contrast to the comparisons described above for the I-95/Route 1 interchange, these analyses incorporated geosynthetic reinforcement.

The example embankment used for these analyses is the same as the one used by Stewart and Filz (2005) to investigate the influence of clay compressibility on the net load applied by the embankment. The embankment configuration is shown in Figure 11, and the square piles are laid out in a square array to produce an area replacement ratio of 0.11. The material property values used in the analyses are described in detail in Stewart and Filz (2005), and some of the key material characteristics are presented here.

The existing clay between columns was assumed to be normally consolidated, and it was represented using the Modified Cam Clay material model. Values of the compressibility parameter λ were selected to represent values of the compression ratio C_{ec} equal to 0.3 and 0.6 in the comparative axisymmetric and three-dimensional analyses. The embankment fill was represented by a linear-elastic, perfectly plastic material model with the Mohr–Coulomb failure criterion using a friction angle of 35° and a

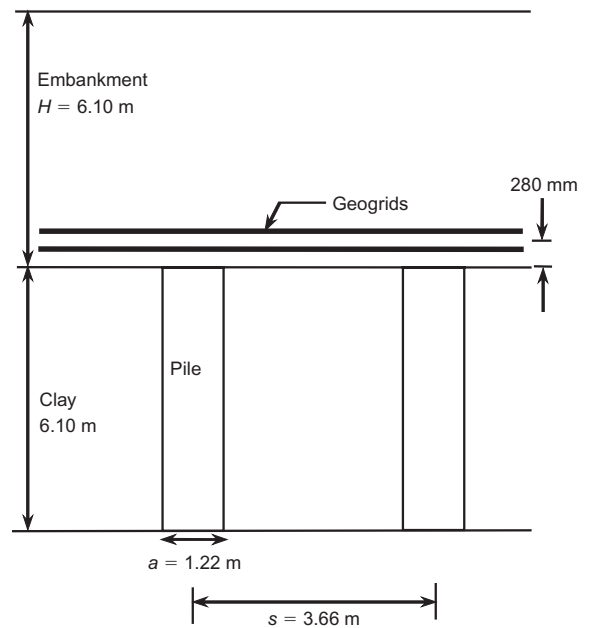


Figure 11. Embankment configuration used for comparison of axisymmetric and three-dimensional analyses

cohesion intercept of zero. The Young's modulus value of the embankment fill was varied from 4800 kPa to 16,800 kPa. The geogrid layers had a combined stiffness, J , of 2040 kN/m.

The results of the analyses are expressed in terms of the net stress reduction ratio SRR_{net} , which is the normalized difference between the average vertical stresses on the top and bottom of the geosynthetic in the area not supported by columns. The normalization is by the average vertical stress from the embankment calculated at the elevation of the geosynthetic. SRR_{net} represents the net vertical stress on the geosynthetic, which is the stress that causes the geosynthetic to deflect downward and develop strain and tension.

The results of the comparative analyses are shown in Table 3, where it can be seen that the average net vertical stresses acting on the geosynthetic in the area not supported by columns are about the same, whether determined from three-dimensional analyses or from axisymmetric analyses.

7. SUMMARY AND CONCLUSIONS

Axisymmetric numerical analyses were performed to model the behavior of geosynthetic-reinforced, column-supported embankments. Drained, axisymmetric finite-

Table 3. Comparison of SRR_{net} values from three-dimensional and axisymmetric analyses

Compression ratio	Embankment modulus (kPa)	SRR_{net}	
		Three-dimensional analyses	Axisymmetric analyses
0.3	4,800	0.32	0.30
0.6	16,800	0.36	0.35

difference and finite-element analyses produced results in good agreement with observed performance and with three-dimensional analyses of the I-95/Route 1 test embankment, which had columnar support but no geosynthetic reinforcement for vertical load transfer. Axisymmetric finite-difference analyses produced results in good agreement with an analytic solution for a pinned disk of membrane material subject to a normal stress producing out-of-plane deformations. The membrane was modeled using two layers of linear-elastic mesh zones of finite thickness. Drained axisymmetric finite-difference analyses produced good agreement with the results of pilot-scale tests performed in Germany to model a geosynthetic-reinforced, column-supported embankment. The basis of comparison for the I-95/Route 1 test embankment and for the pilot-scale model tests was pressure cell readings. The basis of comparison for the axisymmetric membrane was deflection.

Axisymmetric analyses also produced good agreement with three-dimensional analyses for an example column-supported, geosynthetic-reinforced embankment. The basis of comparison in this case was average vertical stress acting on the geosynthetic reinforcement in the area underlain by soil between columns.

These validation studies demonstrate that drained, axisymmetric analyses produce realistic values of the average vertical stresses applied to geosynthetic reinforcement in areas underlain by the soil between columns in column-supported embankments. However, it is understood that full three-dimensional analyses would be necessary to study stress concentrations, such as would be expected at the corner of a square pile cap. Furthermore, the tensile stress and strain distributions that develop in orthotropic geosynthetics in column-supported embankments cannot be determined from axisymmetric analyses. To fully evaluate these effects numerically, three-dimensional modeling is needed.

Thus axisymmetric analyses have been shown to produce realistic values of average vertical stress acting on geosynthetic reinforcement in column-supported embankments. However, axisymmetric analyses are not expected to produce realistic values of tension in the geosynthetic reinforcement. An alternative to performing three-dimensional numerical analyses for the purpose of obtaining the tension in the geosynthetic reinforcement is to first determine the vertical stress acting on the geosynthetic reinforcement using axisymmetric numerical analyses and then use the method in BS 8006 to calculate the tension in the geosynthetic reinforcement.

ACKNOWLEDGMENTS

The authors acknowledge the important contributions of R. Katzenbach, M. Navin, M. Kim and R. Plaut. The authors appreciate the helpful comments provided by the anonymous reviewers. The information presented in this paper is based on work supported by the Virginia Transportation Research Council, the US Department of Education, and the US National Science Foundation, whose support was provided under grant No. CMS-0408281. Any

opinions, findings, conclusions, and recommendations in this paper are those of the authors and do not necessarily reflect the views of the Virginia Transportation Research Council, the US Department of Education or the US National Science Foundation.

NOTATIONS

Basic SI units are given in parentheses:

a	pile cap width (m)
A_s	portion of unit cell not underlain by columns or pile caps (m^2)
C_{ec}	compression ratio (dimensionless)
d_c	diameter of columns or round pile caps (m)
E, E_g	elastic modulus of reinforcement (N/m^2)
J, J_g	reinforcement stiffness (N/m)
K_g	coefficient = $p_{net}A_s/(J_g a)$ (dimensionless)
p	applied uniform vertical load (N/m^2)
p_{net}	average net vertical stress acting on reinforcement (N/m^2)
r	radius of circular membrane (m)
s	center-to-center spacing of columns or pile caps (m)
SRR_{net}	normalized net vertical stress on reinforcement (dimensionless)
t	reinforcement thickness (m)
T_g	tension in reinforcement (N/m)
w_{max}	maximum deflection of membrane (m)
ϵ_g	strain in reinforcement (dimensionless)
η_{crit}	critical shear stress ratio (dimensionless)
κ	Modified Cam Clay swelling parameter (dimensionless)
λ	Modified Cam Clay compressibility parameter (dimensionless)

REFERENCES

- Bentler, D. J., Morrison, C. S., Esterhuizen, J. J. B. & Duncan, J. M. (1999). *SAGE User's Guide: A Finite Element Program for Static Analysis of Geotechnical Engineering Programs*. Center for Geotechnical Practice and Research, Virginia Tech.
- Brinkgreve, R. B. J. & Broere, W. (eds) (2004). *PLAXIS 2D: Version 8*. Delft University of Technology and PLAXIS b.v., the Netherlands.
- BS 8006 (1995). *Code of Practice for Strengthened/Reinforced Soils and Other Fills*. BSI, Milton Keynes.
- Collin, J. G. (2004). Column supported embankment design considerations. *Proceedings of the 52nd Annual Geotechnical Engineering Conference*, University of Minnesota, St. Paul, J. F. Labuz and J. G. Bentler (eds), pp. 51–78.
- Filz, G. M. & Smith, M. E. (2006). *Design of Bridging Layers in Geosynthetic-reinforced, Column-supported Embankments*. Contract Research Report, Virginia Transportation Research Council, Charlottesville.
- Habib, H. A. A., Brugman, M. H. A. & Uijting, B. G. J. (2002). Widening of Road N247 founded on a geogrid-reinforced mattress on piles. *Proceedings of the 7th International Conference on Geosynthetics*, Nice, pp. 369–372.
- Han, J. & Gabr, M. A. (2002). Numerical analysis of geosynthetic-reinforced and pile-supported earth platforms over soft soil. *Journal of Geotechnical and Geoenvironmental Engineering*, **128**, No. 1, 44–53.
- Horgan, G. J. & Sarsby, K. W. (2002). The arching effect of soils over voids and piles incorporating geosynthetic reinforcement. *Proceed-*

- ings of the 7th International Conference on Geosynthetics, Nice, pp. 373–378.
- Itasca Consulting Group (2002a). *FLAC3D: Fast Lagrangian Analysis of Continua in 3 Dimensions*. Itasca Consulting Group, Minnesota, MN, USA.
- Itasca Consulting Group (2002b). *FLAC: Fast Lagrangian Analysis of Continua*. Itasca Consulting Group, Minnesota, MN, USA.
- Kempfert, H.-G., Gobel, C., Alexiew, D. & Heitz, C. (2004) German recommendations for reinforced embankments on pile-similar elements. *EuroGeo3: 3rd European Geosynthetics Conference, Geotechnical Engineering with Geosynthetics*, Munich, pp. 279–284.
- Kempton, G., Russell, D., Pierpoint, N. D. & Jones, C. J. F. P. (1998). Two- and three-dimensional numerical analysis of the performance of piled embankments. *Proceedings of the 6th International Conference on Geosynthetics*, Atlanta, GA, USA, pp. 767–772.
- Rogbeck, Y., Gustavsson, S., Sodergren, I. & Lindquist, D. (1998). Reinforced piled embankments in Sweden: design aspects. *Proceedings of the 6th International Conference on Geosynthetics*, pp. 755–762.
- Russell, D., Naughton, P. J. & Kempton, G. (2003) A new design procedure for piled embankments. *Proceedings of the 56th Canadian Geotechnical Conference and the NAGS Conference*, Winnipeg, MB, pp. 858–865.
- Russell, D. & Pierpoint, N. (1997). An assessment of design methods for piled embankments. *Ground Engineering*, **30**, No. 11, 39–44.
- Stewart, M. E., Navin, M. P. & Filz, G. M. (2004). Analysis of a column-supported test embankment at the I-95/Route 1 interchange. *Proceedings of Geo-Trans 2004, Geotechnical Engineering for Transportation Projects*, Los Angeles, CA, USA, ASCE, pp. 1337–1346.
- Stewart, M. E. & Filz, G. M. (2005). Loads on geosynthetic reinforcement in bridging layers for pile-supported embankments. *Proceedings of Geo-Frontiers 2005*, ASCE, Austin.
- Ugural, A. C. (1999). *Stresses in Plates and Shells*. McGraw-Hill, Boston, MA, 502 pp.
- Zaeske, D. (2001). Zur Wirkungsweise von unbewehrten und bewehrten mineralischen Tragschichten über pfahlartigen Gründungselementen. *Schriftenreihe Geotechnik*, Universität Gh-Kassel, Heft 10.

The Editors welcome discussion on all papers published in *Geosynthetics International*. Please email your contribution to discussion@geosynthetics-international.com by 15 August 2007.